Chemical and Electrochemical Redox Behavior of 9-Anthrylmethyl-Functionalized η^5-Cyclopentadienyl Derivatives of Rhodium(I) and Iridium(I): Generation and EPR Characterization of the Corresponding Cation Radicals

Maurizio Carano,[†] Francesca Cicogna,[‡] Irene D'Ambra,[‡] Benedetta Gaddi,[‡] Giovanni Ingrosso,*[,‡] Massimo Marcaccio,[†] Demis Paolucci,[†] Francesco Paolucci,*[,†] Calogero Pinzino,*[,§] and Sergio Roffia[‡]

Dipartimento di Chimica 'G. Ciamician', Università di Bologna, Via Selmi 2, 40126 Bologna, Italy, Dipartimento di Chimica e Chimica Industriale, Università di Pisa, Via Risorgimento 35, 56126 Pisa, Italy, and Istituto per i Processi Chimico-Fisici del CNR, Area della Ricerca di Pisa, Via G. Moruzzi 1, 56124 Pisa, Italy

Received July 26, 2002

The study of the electrochemical behavior (CV) of 9-anthrylmethylcyclopentadienyl ($AnCH_2C_5H_4$) derivatives of rhodium(I) and iridium(I) of formula [M(η^5-$AnCH_2C_5H_4$)L_2] (M = Rh or Ir; L = η^2-C_2H_4, η^1-CO, η^2-C_8H_{14}, PPh_3; L_2 = η^4-C_8H_{12}), **1**−**8**, in strictly aprotic conditions, allows a satisfactory interpretation of the observed electrode processes and gives information about the location of the redox sites along with the thermodynamic characterization of the corresponding redox processes. These data show that the occurrence of an intramolecular charge-transfer process between the photoexcited 9-anthryl group and the cyclopentadienylmetal unit is a possible route for the observed anthracenic fluorescence quenching in the compounds **1**−**8**. Moreover, a study was carried out on the redox behavior of these complexes under chemical activation. The one-electron oxidation of compounds **1**−**8** by thallium(III) trifluoroacetate leads to the formation of the corresponding cation radicals, whose highly resolved X-band EPR spectra were fully interpreted by computer simulation as well as by semiempirical and DFT calculations of spin density distribution.

1. Introduction

Several cyclopentadienyl derivatives of group 9 transition metals in the oxidation state +1 of formula [$MCpL_2$] exhibit excellent nucleophilic properties, and by reacting with electrophiles, they can behave as metal bases or as one-electron reductants, thus giving rise to the corresponding 17e$^-$ cation radicals (Scheme 1).[1]

As far as the formation of acid−base adducts of the type **1** (Scheme 1) is concerned, a pioneering observation was done by Wilkinson et al., who found that [Co(η^5-C_5H_5)$(CO)_2$] decomposes rapidly by reacting with Brønsted acids.[2] Five years later, Kemmitt et al. succeeded in isolating the compound [Co(η^5-C_5H_5)$(CO)_2(HgCl_2)$] from the reaction of [Co(η^5-C_5H_5)$(CO)_2$] with $HgCl_2$, thus providing the first evidence for the direct interaction between the basic cobalt(I) center and an acid.[3] From that time a variety of cyclopentadienylmetal−Lewis acid adducts have been isolated.[4,5]

Scheme 1

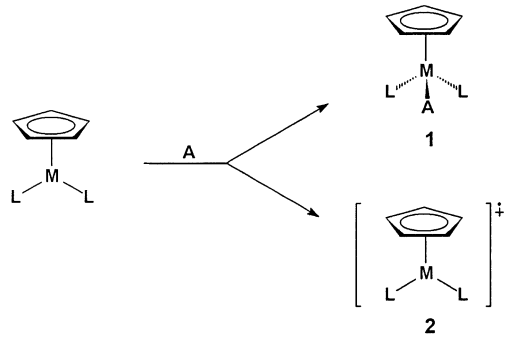

As for the generation of species such as **2** (Scheme 1), the cultural contribution given by McKinney,[6] Connelly,[7] Geiger,[8] Gennett,[9] and Sutton[10] is of great relevance. Accordingly, the chemical and electrochemical one-electron oxidation of complexes of the type [$MCpL_2$] (M = Co, Rh, Ir; Cp = η^5-C_5H_5 or η^5-C_5Me_5) is generally agreed to implicate the formation of the corresponding 17-electron cation radicals, whose chemistry has aroused great interest.[11] However, only in a few cases were these species sufficiently stable to be

* To whom correspondence should be addressed. E-mail: vanni@dcci.unipi.it (G.I.); paolucci@ciam.unibo.it (F.P.); rino@indigo.icqem.pi.cnr.it (C.P.).
[†] Università di Bologna.
[‡] Università di Pisa.
[§] Istituto per i Processi Chimico-Fisici del CNR.

(1) (a) Shriver, D. *Acc. Chem. Res.* **1970**, *3*, 231. (b) Werner, H. *Angew. Chem., Int. Ed. Engl.* **1983**, *22*, 927. (c) Horwitz, C. P.; Shriver, D. F. *Adv. Organomet. Chem.* **1984**, *23*, 219. (d) Angelici, R. J *Acc. Chem. Res.* **1995**, *28*, 51.

(2) Davison, A.; McFarlane, W.; Pratt, L.; Wilkinson, G. *J. Chem. Soc.* **1962**, 3653.

(3) Cook, D. J.; Dawes, J. L.; Kemmitt, R. D. W. *J. Chem. Soc. A* **1967**, 1547.

10.1021/om020607j CCC: $22.00
Publication on Web 11/08/2002

Scheme 2

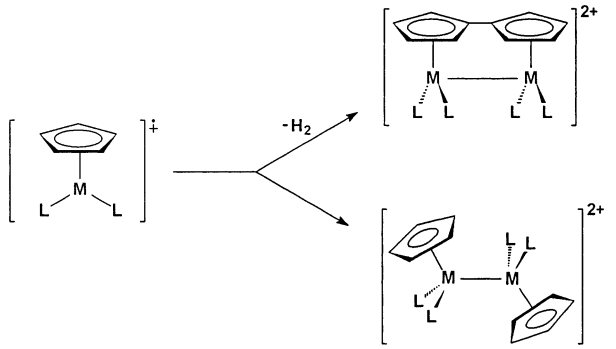

isolated or studied by EPR.[12,13] Typically, these organometallic cations undergo a dimerization reaction that can take place at the cyclopentadienyl site, thus giving rise to a dicationic complex in which two metal centers are coordinated to the fulvalene dianion,[14] or may implicate a metal−metal coupling reaction (Scheme 2).[15] Moreover, in some cases the reaction between cyclopentadienyl-metal bases and Lewis acids can be accompanied by complex self-assembling processes that result in the formation of quite exotic structures.[16]

Some of us have recently reported the synthesis and a study of the photophysical properties of some 9-anthrylmethyl-functionalized η^5-cyclopentadienyl derivatives of rhodium(I) and iridium(I), **1**−**5**, **7**, and **8**.[17] The synthesis and characterization of **6** is reported in this paper.

It has been shown that the cyclopentadienylmetal moiety is capable of modifying the photophysical properties characteristic of the anthryl group, whose fluorescence is strongly quenched in all cases.[17] The occurrence of an intramolecular electron transfer between the photoexcited anthryl group and the cyclopentadienylmetal moiety was suggested as a likely mechanism for the anthryl fluorescence quenching,[17] as already shown in the case of the bimetallic rhodium(I) derivatives **9**.[18]

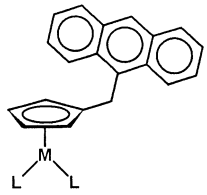

1: M = Rh; L = η^2-C_2H_4

2: M = Rh; L = η^1-CO

3: M = Rh; L = η^2-C_8H_{14}

4: M = Rh; L = PPh_3

5: M = Rh; L_2 = η^4-C_8H_{12}

6: M = Ir; L = η^1-CO

7: M = Ir; L = η^2-C_8H_{14}

8: M = Ir; L_2 = η^4-C_8H_{12}

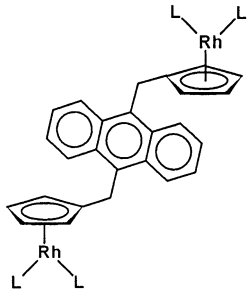

9

L = olefins or CO

On this basis, a study of the redox behavior of complexes **1**−**8** was started with the aim to acquire a deeper insight into their photophysical behavior. The study, reported in this paper, has led to significant results. On one hand, the thermodynamic requirements,

(4) (a) Dawes, J. L.; Kemmitt, R. D. W. *J. Chem. Soc. A* **1968**, 1072. (b) Chalmers, A. A.; Lewis, J.; Wild, S. B. *J. Chem. Soc. A* **1968**, 1013. (c) Edgar, K.; Johnson, B. F. G.; Lewis, J.; Wild, S. B. *J. Chem. Soc. A* **1968**, 2851. (d) Nowell, I. W.; Russell, D. R. *J. Chem. Soc., Dalton Trans.* **1972**, 2393. (e) Intille, G. M.; Braithwite, M. J. *J. Chem. Soc., Dalton Trans.* **1972**, 645. (f) Brotherton, P. D.; Raston, C. L.; White, A. H.; Wild, S. B. *J. Chem. Soc., Dalton Trans.* **1976**, 1799. (g) Rossell, O.; Seco, M.; Torra, I.; Solans, X.; Font-Altaba, M. *J. Organomet. Chem.* **1984**, *270*, C36. (h) Bruno, G.; Lo Schiavo, S.; Piraino, P.; Faraone, F. *Organometallics* **1985**, *4*, 1098. (i) Field, J. S.; Haines, R. J.; Meintjies, E.; Sigwarth, B.; Van Rooyen, P. H. *J. Organomet. Chem.* **1984**, *268*, C43. (j) Einstein, F. W. B.; Pomeroy, R. K.; Raushman, P.; Willis, A. C. *Organometallics* **1985**, *4*, 250. (k) Einstein, F. W. B.; Glavina, P. G.; Pomeroy, R. K.; Rushman, P.; Willis, A. C. *J. Organomet. Chem.* **1986**, *317*, 255. (l) Della Pergola, R.; Demartin, F.; Garlaschelli, L.; Monassero, M.; Martinego, S.; Masciocchi, N.; Sansoni, M. *Organometallics* **1981**, *10*, 2239. (m) Cabeza, J. A.; Fernadez-Colinas, J. M.; Garcia-Granda, S.; Riera, V.; Van der Maelen, J. F. *Inorg. Chem.* **1992**, *31*, 1233.

(5) (a) Burlicht, J. M. In *Comprehensive Organometallic Chemistry*; Wilkinson, G., Stone, F. G. A., Abel, E. W., Eds.; Pergamon: Oxford, 1982; Vol. 6, p 983. (b) Rosenberg, E.; Hardcastle, K. I. In *Comprehensive Organometallic Chemistry*; Wilkinson, G., Stone, F. G. A., Abel, E. W., Eds.; Pergamon: Oxford, 1995; Vol. 6, p 323.

(6) (a) McKinney, R. J. *J. Chem. Soc., Chem. Commun.* **1980**, 603. (b) McKinney, R. J. *Inorg. Chem.* **1982**, *21*, 2051. (c) Harlow, R. L.; McKinney, R. J.; Whitney, J. F. *Organometallics* **1983**, *2*, 1839.

(7) (a) Connelly, N. G.; Lucy, A. R.; Galas, A. M. R. *J. Chem. Soc., Chem. Commun.* **1981**, 43. (b) Connelly, N. G.; Lucy, A. R.; Payne, J. D.; Galas, A. M. R.; Geiger, W. E. *J. Chem. Soc., Dalton Trans.* **1983**, 1879. (c) Broadly, K.; Connelly, N. G.; Geiger, W. E. *J. Chem. Soc., Dalton Trans.* **1983**, 121. (d) Connelly, N. G.; Freeman, M. J.; Manners, I.; Guy Orpen, A. *J. Chem. Soc., Dalton Trans.* **1984**, 2703. (e) Connelly, N. G.; Raven, S. J. *J. Chem. Soc., Dalton Trans.* **1986**, 1613. (f) Brammer, L.; Connelly, N. G.; Edwin, J.; Geiger, W. E.; Guy Orpen, A.; Sheridan, J. B. *Organometallics* **1988**, *7*, 1259.

(8) (a) Moraczewski, J.; Geiger, W. E. *J. Am. Chem. Soc.* **1981**, *103*, 4779. (b) Fonseca, E.; Geiger, W. E.; Bitterwolf, T. E.; Rheingold, A. L. *Organometallics* **1988**, *7*, 567.

(9) Gennett, T.; Grzeszczyk, E.; Jefferson, A.; Sidur, K. M. *Inorg. Chem.* **1987**, *26*, 1856.

(10) Einstein, F. W. B.; Jones, R. H.; Zhang, X.; Yan, X.; Nagelkerke, R.; Sutton, D. *J. Chem. Soc, Chem. Commun.* **1989**, 1224.

(11) (a) Baird, M. C. *Chem. Rev.* **1988**, *88*, 1217. (b) Trogler, W. C. *Organometallic Radical Processes*; Elsevier: Amsteram, 1990.

(12) (a) McKinney, R. J. *Inorg. Chem.* **1982**, *21*, 2051. (b) Harlow, R. L.; McKinney, R. J.; Whitney, J. F. *Organometallics* **1983**, *2*, 1839. (c) Connelly, N. G.; Raven, S. J. *J. Chem. Soc., Dalton Trans.* **1986**, 1613. (d) Broadly, K.; Connelly, N. G.; Geiger, W. E. *J. Chem. Soc., Dalton Trans.* **1983**, 121.

(13) (a) Astruc, D. *Electron Transfer and Radical Processes in Transition-Metal Chemistry*; VCH Publishers: New York, 1995. (b) Connelly, N. G.; Geiger, W. E. *Chem. Rev.* **1996**, *96*, 877.

(14) De Azevedo, C. G.; Vollhardt, K. P. C. *Synlett* **2002**, 1019.

(15) (a) Haines, R. J. In *Comprehensive Organometallic Chemistry*, 2nd ed.; Shriver, D. F., Bruce, M. I., Eds.; Pergamon Press: New York, 1995; Vol. 7, Chapter 11. (b) Bitterwolf, T. E. *Coord. Chem. Rev.* **2000**, *206*−*207*, 419.

(16) (a) Chiaradonna, G.; Ingrosso, G.; Marchetti, F. *Angew. Chem., Int. Ed.* **2000**, *39*, 3872. (b) Gade, L. H. *Angew. Chem., Int. Ed. Engl.* **1993**, *32*, 24. (c) Rosemberg, E.; Hardcastle, K. I. In *Comprehensive Organometallic Chemistry*, Abel, E. W., Stone, F. G. A., Wilkinson, G., Eds.; Pergamon: Oxford, 1995; Vol. 10, p 323. (d) Gade, W.; Weiss, W. *Angew. Chem., Int. Ed. Engl.* **1981**, *20*, 803.

(17) Cicogna, F.; Colonna, M.; Houben, J. L.; Ingrosso, G.; Marchetti, F. *J. Organomet. Chem.* **2000**, *593*−*594*, 251.

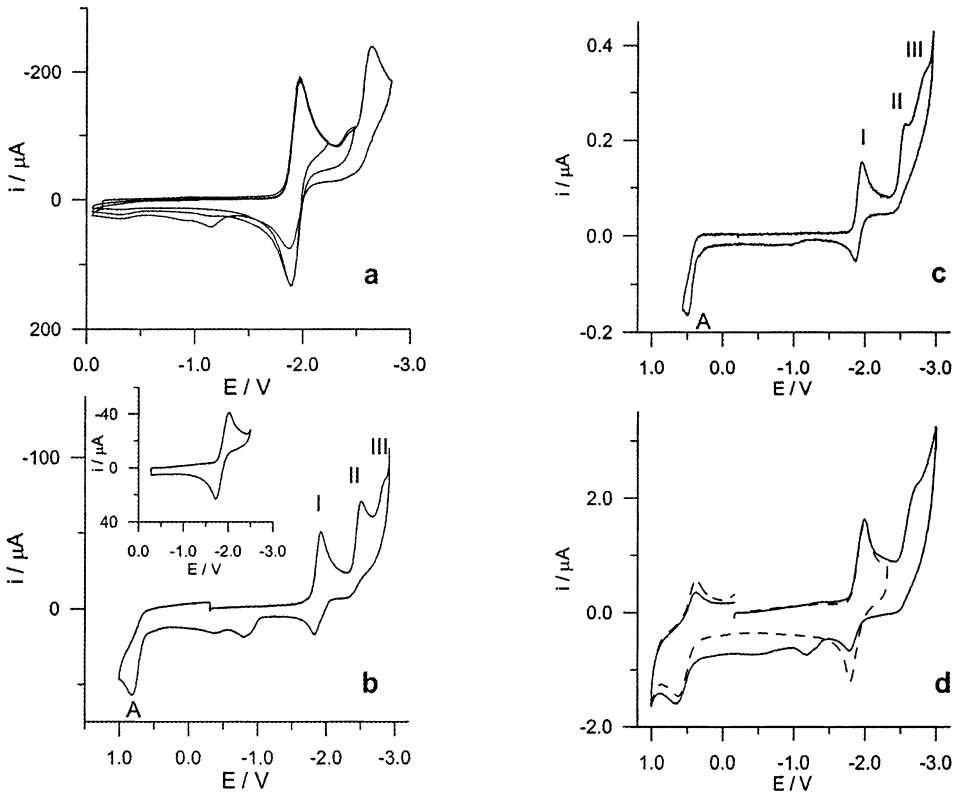

Figure 1. CV curves obtained in 0.05 M TBAH THF solutions, at 25 °C: (a) 9-anthrylmethylcyclopentadiene, 2.0 mM, v = 0.5 V/s, working electrode Pt wire; (b) [Rh(η^5-AnCH$_2$C$_5$H$_4$)(η^2-C$_2$H$_4$)$_2$] **1**, 1.0 mM, v = 0.5 V/s, working electrode Pt wire; (c) [Rh(η^5-AnCH$_2$C$_5$H$_4$)(η^2-C$_8$H$_{14}$)$_2$] **3**, 2.0 mM, v = 1 V/s, working electrode Pt disk 125 μm diameter; (d) [Rh(η^5-AnCH$_2$C$_5$H$_4$)-(η^2-C$_8$H$_{14}$)$_2$] **3**, 2.0 mM, v = 100 V/s, working electrode Pt disk 125 μm diameter.

needed to substantiate the occurrence of the suggested[17] intramolecular electron transfer as responsible for the anthracene fluorescence quenching, are completely satisfied on the basis of the results of the study of the electrochemical behavior (CV) of **1**−**8**. On the other hand, it has been shown that, by reacting with thallium(III) trifluoroacetate, a strongly oxidant Lewis acid, these complexes undergo one-electron oxidation, thus giving rise to the corresponding cation radicals that were characterized through their EPR spectra as well as by DFT or PM3 semiempirical calculation of their spin density distribution. The electronic features exhibited by these cation radicals account nicely for the reactivity outlined in Scheme 2.

2. Results and Discussion

2.1. Electrochemical Studies. Figure 1a shows the CV curve for a 2.0 mM solution of 9-anthrylmethylcyclopentadiene, which was assumed to be a suitable model for the anthrylic unit in species **1**−**8**.

Two reduction processes are observed: the first peak is reversible, with $E_{1/2}$ = −1.93 V, and the second one is irreversible (E_p = −2.65 at 0.5 V/s). The first peak became less reversible (i.e., the anodic-to-cathodic peak ratio, i_{pa}/i_{pc}, became less than 1) when the second peak was also included in the forward scan (Figure 1a). Furthermore, two small anodic peaks at ca. −0.9 and −1.1 V were observed in the reverse scan following the second irreversible reduction. Such oxidation processes were attributed to electroactive species emerging from the chemical degradation of the dianion of 9-anthrylmethylcyclopentadiene, in line with the electrochemical behavior of anthrylic derivatives carrying electron-donating groups.[18b]

The CV curve for a 1.0 mM THF solution of **1** is shown in Figure 1b. Three reduction peaks are observed, denoted by roman numbers. Analogously to 9-anthrylmethylcyclopentadiene, peak I is reversible ($E_{1/2}$ = −1.89 V) when the potential scan is inverted before peak II (Figure 1b, inset); otherwise a less-than-one i_{pa}/i_{pc} was found. Peaks II and III were irreversible at any scan rate investigated (≤1000 V/s), and their E_p (at 0.5 V/s) were −2.62 and −2.78 V, respectively. Furthermore, such peaks shifted to more negative potentials by approximately 30 mV for a 10-fold increase of scan rate, suggesting that their irreversibility is due to the occurrence of a fast chemical reaction following the reduction process (EC mechanism). Both peaks I and II correspond to one-electron processes, as determined by chronoamperometric experiments at ultramicroelectrodes,[18c] and by analogy with the model 9-anthrylmethylcyclopentadiene, they were attributed to the subsequent reductions of the anthrylic unit. Only a minor shift of the two processes is observed in **1** with respect to 9-anthrylmethylcyclopentadiene, which suggests that little or no interaction occurs in the ground state between the anthrylic unit and the metal-containing

(18) (a) Carano, M.; Careri, M.; Cicogna, F.; D'Ambra, I.; Houben, J. L.; Ingrosso, G.; Marcaccio, M.; Paolucci, F.; Pinzino, C.; Roffia, S. *Organometallics* **2001**, *20*, 3478. (b) Heinze, J. In *Organic Electrochemistry*; Lund, H., Hammerich, O., Eds.; M. Dekker: New York, 2001; p 293. (c) Cecchet, F.; Gioacchini, A. M.; Marcaccio, M.; Paolucci, F.; Roffia, S.; Alebbi, M.; Bignozzi, C. A. *J. Phys, Chem. B* **2002**, 106, 3926, and references therein.

Table 1. CV Parameters for Compounds 1−8[a]

compound	oxidation	reduction	ΔG (eV)[b]
9-anthrylmethylcyclopentadiene		−1.91[d]; −2.65[c]	
[Rh(η^5-AnCH$_2$C$_5$H$_4$)(η^2-C$_2$H$_4$)$_2$] **1**	0.98[c] (Rh)	−1.89[d] (An); −2.62[c] (An)	−0.83
[Rh(η^5-AnCH$_2$C$_5$H$_4$)(CO)$_2$] **2**	1.01[c] (Rh)	−1.85[c] (Rh); −1.98[d] (An); −2.85[c] (An)	−0.75
[Rh(η^5-AnCH$_2$C$_5$H$_4$)(η^2-C$_8$H$_{14}$)$_2$] **3**	0.51[d] (Rh)	−1.91[d] (An); −2.54[c] (An)	−1.28
[Rh(η^5-AnCH$_2$C$_5$H$_4$)(PPh$_3$)$_2$] **4**	−0.08[d] (Rh); 0.90[c] (Rh)	−1.91[d] (An); −2.50[c] (An)	−1.87
[Rh(η^5-AnCH$_2$C$_5$H$_4$)(η^4-C$_8$H$_{12}$)] **5**	0.44[d] (Rh)	−2.11[d] (An); −2.75[c] (An)	−1.15
[Ir(η^5-AnCH$_2$C$_5$H$_4$)(CO)$_2$] **6**	0.85[c] (Ir)	−2.09[d] (An); −2.52[c] (Ir); −3.06[d] (An)	−0.76
[Ir(η^5-AnCH$_2$C$_5$H$_4$)(η^2-C$_8$H$_{14}$)$_2$] **7**	0.65[d] (Ir); 0.95[c] (Ir)	−1.88[d] (An); −2.48[c] (An)	−1.17
[Ir(η^5-AnCH$_2$C$_5$H$_4$)(η^4-C$_8$H$_{12}$)] **8**	0.48[d] (Ir)	−2.07[d] (An); −2.46[c] (An)	−1.15

[a] V vs SCE, T = 25 °C. The localization of the redox process is given in parentheses. [b] ΔG, driving force for the photoinduced intramolecular charge transfer (reductive quenching, see text); a correction to the CS state energy of −0.5 eV was introduced for taking into account ion−solvent interactions (ref 36). [c] E_p (at 0.5 V/s). [d] $E_{1/2}$. [e] $E_{1/2}$ from simulation.

moiety. Peak III is partially superimposed to the solvent-electrolyte discharge current, making the evaluation of the number of electrons associated to it difficult. Such a peak however shifted greatly toward more negative potentials as the scan rate was increased and was no longer observed at $v \geq 200$ V/s (vide infra). Attribution of such a peak to a metal-centered reduction process was not supported by the results of a CV investigation performed, under similar conditions, on (η^5-cyclopentadienyl)bis(η^2-ethylene)rhodium(I), for which no reduction process is observed up to −3.0 V, in line with previously reported studies.[19] In the positive potential region a single one-electron chemically irreversible oxidation process was observed, with E_p = 0.98 V (at 0.5 V/s), Figure 1b. The reversibility of the oxidation peak was not obtained at scan rates up to 1000 V/s. Such a process was attributed to a metal-centered oxidation, since 9-anthrylmethylcyclopentadiene did not show any oxidation process within the THF available positive potential window.

The above description of the redox properties of **1** in terms of reductions prevalently located on the anthrylic unit and of oxidations prevalently located on the metal center was also found to describe adequately the electrochemical behavior of complexes **3**−**6** and **8**, which showed CV patterns closely resembling that of **1**. Figure 1c shows, for instance, the CV curve for a 2.0 mM **3**·THF solution. Three cathodic peaks (I−III) and one oxidation peak (A) are observed analogously to what was observed for **1**. Still, peak I is reversible while peaks II, III, and A are irreversible, under the condition of Figure 1c (v = 1 V/s). However, at variance with **1**, peak A became reversible, with $E_{1/2}$ = 0.51 V, at a scan rate ≥ 100 V/s (Figure 1d), thus suggesting that the follow-up chemical reaction coupled to the oxidation process is slower in the case of **3** than in **1**. Figure 1d also shows that, as anticipated above in the case of **1**, peak III is no longer observed at relatively high scan rates, suggesting that such a reduction process might be associated with a product deriving from the degradation of the anthryl-centered dianion.

Notice that only small changes of the anthryl-centered reduction potentials (Table 1) were observed along the series of compounds, despite the large variation of the electron-donor properties of the ancillary ligands. This substantiates the above hypothesis that little or no interaction between the metal-containing moiety and the reduced anthrylic unit would occur in the ground state. This conclusion was also supported by the observation that even the replacement of rhodium by iridium does not bring about a significant change in the reduction behavior of the complex. By contrast, and not unexpectedly, the anodic behavior of the complexes was found to vary to a much greater extent while changing the donor−acceptor properties of the ancillary ligands. In particular, the stronger the electron-donor properties of such ligands, the easier the oxidation of the metal center. Indeed, the potential of metal-centered oxidation decreases in the order CO > C_2H_4 > C_8H_{14} > C_8H_{12} > PPh_3, independently of the metal (Table 1). Moreover, along with the increasing of the shift of the first oxidation peak toward less positive potentials, an increased reversibility of the redox process was found: a reversible oxidation was found, in the case of **4**, at scan rates as slow as 0.1 V/s, at $v \geq 100$ V/s for **3**, and it was still irreversible at v = 1000 V/s in **1**. Finally, both in the case of the bis(cyclooctene)iridium complex **7** and in that of the bis(triphenylphosphine)-rhodium complex **4**, a second, irreversible metal-centered oxidation was observed at more positive potentials (Table 1).

Dicarbonyl complexes **2** and **6** deserve a separate analysis because, in these cases, metal-centered reduction processes were also observed at odds with the previous complexes and a significant interaction between metal-containing and anthrylic moieties was evidenced.The CV curve of (dicarbonyl)rhodium complex **2** is shown in Figure 2a. Similarly to the previous species, two main reduction peaks are observed. Peak II corresponds to the exchange of one electron and is totally irreversible (E_p = −2.85 V). The first peak, by contrast, is the result of the superimposition of two subsequent reduction processes, namely, I′ and I, occurring at very close potentials. Peak I′ shifted toward more negative potentials by ca. 30 mV for a 10-fold increase of scan rate, eventually coalescing with peak I at $v \geq 200$ V/s. At v = 1000 V/s, a reversible peak was observed (Figure 2a, dashed line), whose height corresponded approximately to twice that of peak II. Digital simulation of the CV curve finally confirmed that peaks I and I′ correspond to two subsequent one-electron diffusion-controlled reductions, with $E_{1/2}$ = −1.92 and −1.98 V, respectively. While the second of such reductions is chemically and electrochemically reversible, the first one (peak I′) is followed by a fast (rate constant ≈ 10^3 s^{-1}) chemical reaction. By comparison with the previous complexes, the reversible process, as well as the irreversible peak at −2.85 V, can confidently be

(19) Dessy, R. E.; Stary, F. E.; King, R. B.; Waldrop, M. *J. Am. Chem. Soc.* **1966**, *88*, 471.

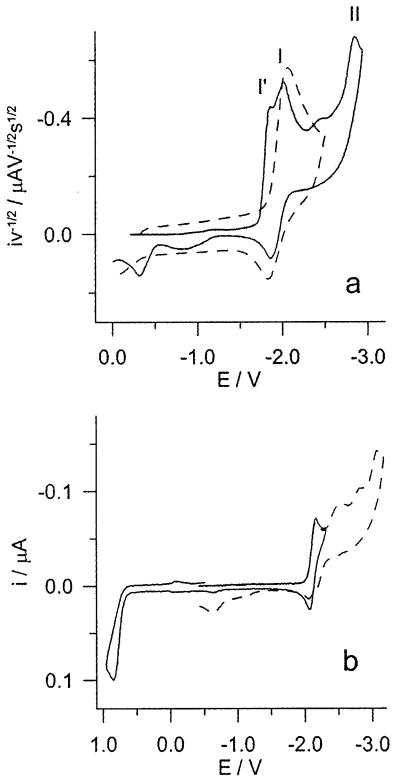

Figure 2. CV curves obtained in 0.05 M TBAH THF solutions, at 25 °C; v = 0.5 V/s: (a) [Rh(η^5-$AnCH_2C_5H_4$)$(CO)_2$] **2**, 2.0 mM, v = 0.5 V/s (full line) or v = 1000 V/s (dashed line), working electrode Pt disk 125 mm diameter; (b) [Ir(η^5-$AnCH_2C_5H_4$)$(CO)_2$] **6**, 2.0 mM, v = 0.5 V/s, working electrode Pt disk 125 mm diameter.

attributed to the reduction of the anthrylic unit of **2**. The irreversible reduction at −1.85 V (peak I′) is therefore likely to involve the metal-containing unit. The attribution of the latter process to the metal-containing unit was also confirmed by comparison with the CV behavior of the model complex [Rh(η^5-C_5H_5)$(CO)_2$].

In the positive potentials, region **2** shows an irreversible one-electron oxidation peak located at 1.01 V, attributed to a metal-centered oxidation. The process is significantly shifted toward more positive potentials with respect to the model compound [Rh(η^5-C_5H_5)$(CO)_2$]. This might be indicative of a strong interaction of the metal-containing unit with the anthrylic moiety. Such an interaction may also explain the increased stability toward rhodium-to-Cp cleavage observed upon reduction of the metal-containing moiety in **2** with respect to [Rh(η^5-C_5H_5)$(CO)_2$]. It has been observed indeed that the 9-anthrylmethylcyclopentadienyl ligand is a better electron donor than cyclopentadienyl.[17]

An analogous behavior was found in the case of (dicarbonyl)iridium homologue **6**. The CV curve of **6** in the region of negative potentials, shown in Figure 2b, displays four subsequent reduction processes. Only the first peak is reversible, with $E_{1/2}$ = −2.09 V, and is attributed, together with the irreversible peak at −3.06, to the anthrylic unit. The second peak (E_p = −2.52 V) was then attributed to the one-electron irreversible reduction of the metal-containing unit. A follow-up chemical reaction coupled to such a process would be responsible for both the irreversibility of the CV peak and the appearance of the third peak (at −2.81 V). Such an attribution of the metal-centered process was confirmed by comparison with the CV curve of the model compound, [Ir(η^5-C_5H_5)$(CO)_2$]. Finally, in the positive potentials region, **6** undergoes an irreversible one-electron oxidation process (Figure 2b), with E_p = 0.85 V, also attributed to the metal-containing unit.

Even though a significant interaction between metal-containing and anthrylic moieties seems to occur in **2** on the basis of the comparison with the model compounds, [Rh(η^5-C_5H_5)$(CO)_2$] and 9-anthrylmethylcyclopentadiene, a description of the redox properties of **2**, and likewise of **6**, in terms of localized redox orbitals still seems to hold, allowing to define the observed processes as either metal-centered oxidation and reduction or anthryl-centered reductions.

Finally, in the CV curves of **1**−**8**, oxidation peaks at ca. −0.35 and −0.80 V were observed in the reverse scan when potential was inverted following one of the irreversible cathodic peaks. In analogy with what has been observed through the CV study of [Co(η^5-C_5H_5)$(CO)_2$],[20] which undergoes reductive cleavage of the cobalt-to-Cp bond, under conditions similar to those adopted in this work, we are strongly inclined to attribute such anodic peaks to the oxidation of the 9-anthrylmethylcyclopentadienyl free ligand, which would be analogously released from the reduced complex, thus also explaining the irreversibility of the metal-centered reduction.

2.2. Photoinduced Electron Transfer. In a previous report,[17] the preliminary results of the present electrochemical study were used for substantiating the hypothesis that the strong quenching of the anthryl-based fluorescence observed for complexes **1** and **2** might be due to the intramolecolar charge transfer between the excited anthryl unit and the metal-containing moiety, leading to a charge-separated (CS) state. The results of that study are now reappraised and extended to the whole series of species **1**−**8** on the basis of the results of the present CV study, as gathered in Table 1. The thermodynamic requirement that the above intramolecular process be exoergonic may be quantitatively verified by the evaluation of the driving force (ΔG) for the formation of the CS state, given, in a first approximation, by $\Delta G = [e(E_{1/2,D} - E_{1/2,A}) - E_{00}]$. Here $E_{1/2,D}$ and $E_{1/2,A}$ correspond to the donor oxidation and acceptor reduction, respectively, in the anthrylic dyad, and E_{00} is the energy of its anthryl-based excited state. In addition, the solvent effect on the energy of the CS state can be quantified with the help of the Born formula. This model handles the CS radical pair as two spherical ions separated by a distance, submerged into a solvent considered as a continuum, and predicts a strong impact of the solvent polarity on the driving force for the intramolecular electron-transfer reaction (Rehm−Weller). By using the $E_{1/2}$ (and E_p) values and the maximum in the fluorescence spectrum of 9-anthrylmethylanthracene as E_{00} (ca. 3.2 eV), and introducing a correction for the ion−solvent interaction of −0.5 eV for all the species, the evaluated ΔG for the CS process implying an electron-transfer process from the metal-containing moiety to the antryl-based photoexcited state

(20) (a) Connelly, N. G.; Geiger, W. E.; Lane, G. A.; Raven, S. J.; Reiger, P. H. *J. Am. Chem. Soc.* **1986**, *108*, 6219. (b) Schore, N. F.; Ilenda, C. S.; Bergman, R. G. *J. Am. Chem. Soc.* **1977**, *99*, 1781.

Scheme 3

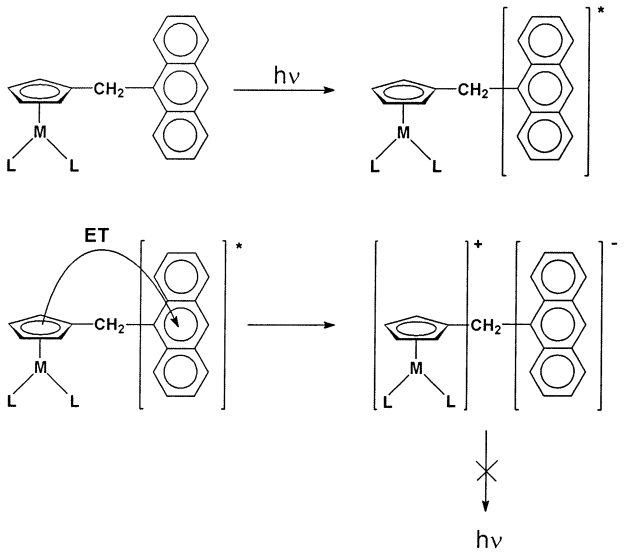

(reductive quenching) (Scheme 3) (Table 1) indicates that such a process may indeed justify the observed strong quenching of the anthracene-based emission in **1**−**8**.

2.3. Chemical Oxidation of Complexes 1−8: EPR Studies and DFT and PM3 Semiempirical Calculations. As shown above, complexes **1**−**8** undergo two main redox processes, under electrochemical conditions, i.e., anthryl-centered reductions and metal-centered oxidations, some of these being reversible. Thus, with the aim to get a deeper insight into the electronic structure of the redox products of **1**−**8**, we started to study the reaction of **1**−**8** with oxidants and reductants in the cavity of an EPR spectrometer. We did not succeed in detecting the products that resulted from the reaction of complexes **1**−**8** with several reductants.[13b] Instead, the EPR study of the oxidation of **1**−**8** with thallium(III) trifluoroacetate oxidants led to much more interesting results. It is widely believed that thallium(III) trifluoroacetate in trifluoroacetic acid is probably the best general oxidant−solvent system so far introduced.[21] We have now found that the one-electron oxidation of complexes **1**−**8** to the corresponding cation radicals (eq 1) can be easily performed by using thallium(III) trifuoroacetate in 1,1,1,3,3,3-hexafluoropropan-2-ol (HFP) or in HFP/CH_2Cl_2 mixtures, HFP being a superior solvent for the generation and stabilization of radical cations.[22]

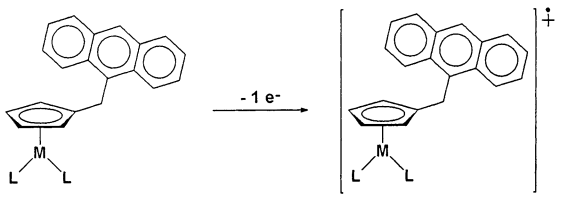

(1)

The intense and well-resolved EPR spectra shown in Figures 3 and 4 have been obtained, at temperatures ranging from −10 to +10 °C, when a frozen solution of the organometallic complex was allowed to warm until a signal appeared. Following the already described procedure,[18,23] the reactants were made to come into contact gradually in the cavity of the EPR spectrometer, under a pure argon atmosphere. Only in the case of complex **5** did we not succeed in obtaining the spectrum of the corresponding cation radical. **5** reacts with HFP, giving rise to a still unknown species, and using only CH_2Cl_2 as the reaction medium, no reaction took place between **5** and thallium(III) trifuoroacetate, even at room temperature.

All the EPR spectra were fully interpreted by computer simulation of the experimental signals.[24] Moreover, DFT calculation of the spin density distribution by using the Spartan 5.1.3. program (Model LSDA/pBP86/DN**)[25−27] allowed a theoretical evaluation of the isotropic hyperfine coupling constants with the various hydrogen nuclei for the cation radicals $\mathbf{1}^+$−$\mathbf{3}^+$ and gave further insight into the electronic structure of such species. For the sake of clarity only the negative spin density is represented in the spin density maps reported in Figures 5. When comparing the theoretical and experimental isotropic hyperfine coupling constants, the limited basis set used, the influence of the solvent, and the vibrational and environmental effects should be take into account in the calculation to produce quite accurate results. Since it is hard to assess the importance of such effects, a semiempirical extrapolation procedure[28] has been adopted to correct the theoretical values and compare them with the experimental ones. Interestingly, the calculated isotropic hyperfine coupling constants for the cation radical $\mathbf{1}^+$−$\mathbf{3}^+$ are in remarkable accordance with those reported above, which were obtained by computer simulation of the experimental spectra of Figure 3 (Table 2).

In the case of the rhodium derivative $\mathbf{4}^+$ and of the iridium derivatives $\mathbf{6}^+$−$\mathbf{8}^+$ the assignments of hyperfine coupling constants were done on the basis of the PM3 semiempirical calculation of the spin density distribution of the cation radicals (Table 2).

The data indicate that in all cases the spin delocalization extends substantially over the 9-anthrylmethylcyclopentadienylmetal moiety. Spin couplings with the nuclei of the ancillary ligands, i.e., η^2-C_2H_4, η^1-CO, η^2-C_8H_{14}, η^4-C_8H_{12}, and PPh_3, if any, should be lower than the observed line widths. According to what is observed in the case of the cation radical of anthracene[29] as well as other studies,[18,30] the highest hyperfine coupling

(21) (a) Elson, I. H.; Kochi, J. K. *J. Am. Chem. Soc.* **1973**, *95*, 5060. (b) Eberson, L.; Hartshorn, M. P.; Persson, O. *J. Chem. Soc., Perkin Trans.* **1995**, 1735.

(22) (a) Eberson, L.; Hartshorn, M. P.; Persson, O. *J. Chem. Soc., Perkin Trans.* **1995**, 1735. (b) Eberson, L.; Hartshorn, M. P.; Persson, O.; Radner, F. *J. Chem. Soc., Chem. Commun.* **1996**, 2105.

(23) (a) Diversi, P.; Forte, C.; Franceschi, M.; Ingrosso, G.; Lucherini, A.; Petri, M.; Pinzino, C. *J. Chem. Soc., Chem. Commun.* **1992**, 1345. (b) Bruni, M.; Diversi, P.; Ingrosso, G.; Lucherini, A.; Pinzino, C.; Raffaelli, A. *J. Chem. Soc., Dalton Trans.* **1995**, 1035. (c) Bruni, M.; Diversi, P.; Ingrosso, G.; Lucherini, A.; Pinzino, C. *Gazz. Chim. Ital.* **1996**, *126*, 239.

(24) Duling, D. R. J. *Magn. Reson. B* **1994**, *104*, 105.

(25) *Spartan* Version 5.1.3; Wavefunction, Inc.: 18401 Von Karman Ave., Suite 370, Irvine, CA 92612.

(26) Beche, A. D. *Phys. Rev. A* **1988**, *38*, 3098.

(27) Perdew, J. P. *Phys Rev. B* **1986**, *33*, 8822.

(28) (a) Fortunelli A.; Salvetti, O. *J. Mol. Struct. (THEOCHEM)* **1993**, *287*, 89 1993; (b) Fortunelli, A. *Int. J. Quantum Chem.* **1994**, *52*, 97.

(29) Carrington, A.; McLachlan, A. D. *Introduction to Magnetic Resonance*; Harper & Row: New York, and John Weatherhill Inc., Tokyo, 1975.

(30) Carano, M.; Cicogna, F.; Houben, J. L.; Ingrosso, G.; Marchetti, F.; Mottier, L.; Paolucci, F.; Pinzino, C.; Roffia, S. *Inorg. Chem.* **2002**, *41*, 3396.

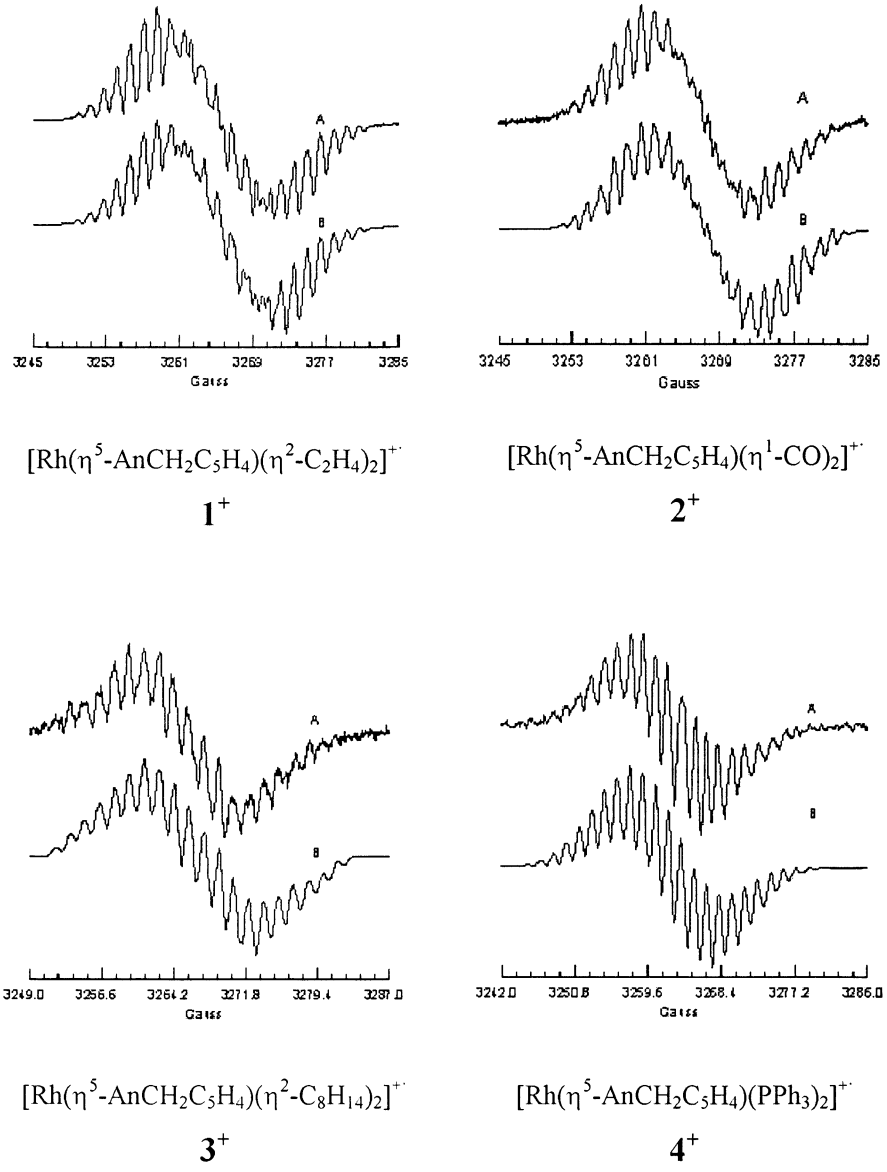

Figure 3. X-band EPR spectra (A, experimental; B, simulated) of the cation radicals derived from rhodium complexes **1**−**4**.

constant is found to be associated with the interaction of electron spin with the nucleus of the hydrogen linked to carbon atom 10 of the 9-anthryl group, in all cases.

That the spin delocalization effects also the metal center, with the only exception of $\mathbf{8}^+$, is unambiguously evident by comparing the EPR spectra of $\mathbf{6}^+$ and $\mathbf{2}^+$ as well as those of $\mathbf{3}^+$ and $\mathbf{7}^+$ (Figures 3 and 4). In fact, the presence of an iridium center ($I = 3/2$) makes the spectra of $\mathbf{6}^+$ and $\mathbf{7}^+$ have a higher complexity, owing to the increased number of lines, if compared with that of the isostructural derivative of rhodium, $\mathbf{2}^+$ and $\mathbf{3}^+$. This is further confirmed by DFT calculations, at least for the rhodium derivatives (Figure 5).

The spin coupling constants with the metal nucleus vary on varying the ancillary ligands. In the case of the rhodium derivatives $\mathbf{1}^+$−$\mathbf{4}^+$, the highest spin-rhodium coupling constant ($a_{Rh} = 3.45$ G) is evaluated for the bis(triphenylphosphine) derivatives $\mathbf{4}^+$. Thus, it is evident that the probability of finding the unpaired electron over the rhodium center is correlated to the electronic effects exerted by the ancillary ligands. Triphenylphosphine, owing to its electron-donor properties, causes an increase of charge density on the rhodium and consequently stabilizes the "partially oxidized metal center". The opposite effect is caused by the π-acid ligands present in the cation radicals $\mathbf{1}^+$−$\mathbf{3}^+$, cyclooctene making the spin delocalization over the rhodium center low. Finally, the spin coupling with rhodium is higher in the case of the bis(ethylene) derivative $\mathbf{1}^+$ than in the dicarbonyl complex $\mathbf{2}^+$.

The trend that is observed in the case of the iridium derivatives $\mathbf{6}^+$−$\mathbf{8}^+$ is less clear. Indeed, the spin-nucleus interaction increases on going from the bis(cyclooctene) derivative $\mathbf{7}^+$ to the dicarbonyl derivative $\mathbf{6}^+$ and, finally, to the cyclooctadiene derivative $\mathbf{8}^+$.

It is to be noticed that the lower the spin coupling constant with the metal center, the higher the spin coupling constants with the anthryl hydrogen nuclei, in all cases. Particularly sensitive to this effect is the hydrogen nucleus on carbon atom 10 of the 9-anthryl group, the highest spin coupling with this nucleus being

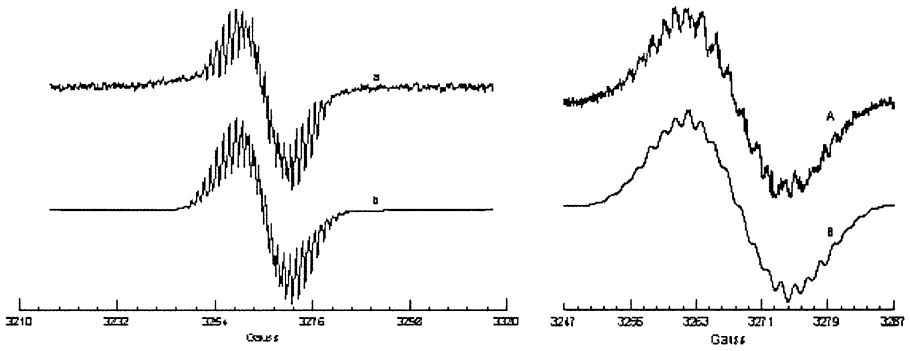

$[Ir(\eta^5\text{-}AnCH_2C_5H_4)(\eta^1\text{-}CO)_2]^{+\cdot}$ $[Ir(\eta^5\text{-}AnCH_2C_5H_4)(\eta^2\text{-}C_8H_{14})_2]^{+\cdot}$

6$^+$ **7**$^+$

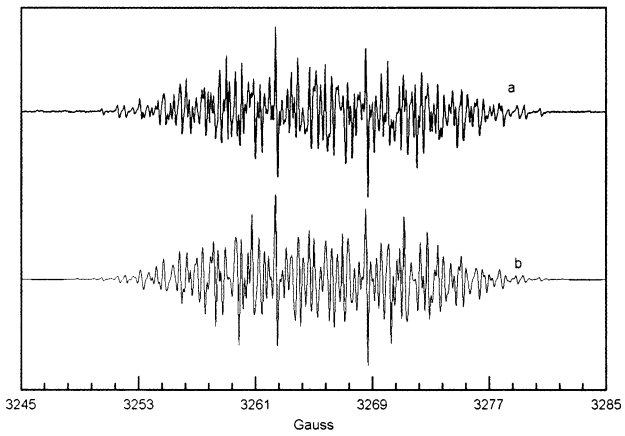

$[Ir(\eta^5\text{-}AnCH_2C_5H_4)(\eta^4\text{-}C_8H_{12})]^{+\cdot}$

8$^+$

Figure 4. X-band EPR spectra (A, experimental; B, simulated) of the cation radicals derived from iridium complexes **6**−**8**.

observed in the case of the cation radicals **8**$^+$, in which case no significant spin coupling with the iridium center is observed.

The conformation of the cation radicals **1**$^+$−**3**$^+$ at the minimum of their energy, as seen from the DFT calculations (Figure 5), and that of the cations **4**$^+$ and **6**$^+$−**8**$^+$, as seen from the PM3 semiempirical calculation of their spin density surface, deserves a final comment. In fact, in all cases the optimized geometry shows the metal center facing the plane of the anthryl group, in a sort of *cisoid* conformation, which probably makes the two moieties involved in a deep electronic communication. The neutral complexes **1** and **2**, in the solid state, exhibit a totally different conformation in which the cyclopentadienylmetal moiety and the anthryl group are on opposite sides (*transoid* conformation).[17] On this basis it could be conjectured that the *cisoid* conformation stabilizes the oxidized form of these complexes to some extent by a possible interaction between the metal center and the π-electrons of the anthryl group, both being electronically poor to some extent as a consequence of the oxidation.

3. Concluding Remarks

In summary, the study of the electrochemical behavior of complexes **1**−**8** allows us to conclude that the occurrence of a vectorial electron transfer from the cyclopentadienylmetal subunit to the photoexcited athryl group is an exoergonic process, and, as such, it can indeed be responsible for the observed anthryl florescence quenching in the case of all complexes **1**−**8**. Some of us have recently shown that an intramolecular electron transfer can be responsible for the anthryl fluorescence quenching observed in the case of 9-anthrylmethyl- or 9-anthroyl-substituted β-ketoenolates of rhodium(III) and iridium(III).[30] In this last case the direction of the most thermodynamically favored electron transfer is inverted; that is, it implies the transfer of one electron from the photoexcited anthryl group to the metal center. In other words, since photoexcited anthracene is either a good electron acceptor or a good electron donor, not unexpectedly the oxidation state of the metal center plays a key role in determining the direction of the electron transfer within the dyads in

Table 2. Experimental and Calculated EPR Data for the Cation Radicals 1^+−3^+,[a] 4^+,[b] and 6^+−8^+ [b]

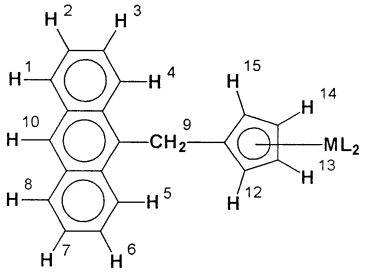

cation radical	T (K)	ΔH_{pp} (G)	exptl and [calcd] hyperfine coupling constants (G) (nucleus)	g_{iso}
$[Rh(\eta^5\text{-}AnCH_2C_5H_4)(\eta^2\text{-}C_2H_4)_2]^{+\bullet}$, $\mathbf{1}^+$	273	0.5	2.31 (Rh); 5.04 (1H); 3.30 (1H); 3.01 (1H); 2.98 (1H); 2.94 (1H); 2.88 (2H); 1.45 (2H); 1.26 (2H); 1.36 (2H) [5.0 (H^{10})]; [3.2 (H^{13} and H^{14})]; [2.9 (H^1 and H^8)]; [2.7 (H^3 and H^6)]; [1.3 (H^4 and H^5)]; [1.2 (H^2 and H^7)]	2.0055
$[Rh(\eta^5\text{-}AnCH_2C_5H_4)(\eta^1\text{-}CO)_2]^{+\bullet}$, $\mathbf{2}^+$	278	0.5	2.12 (Rh); 5.42 (1H); 3.20 (2H); 2.98 (2H); 2.68 (2H); 1.26 (4H) [5.6 (H^{10})]; [3.3 (H^{13} and H^{14})]; [2.8 (H^1 and H^8)]; [2.6 (H^4 and H^5)]; [1.2 (H^3 and H^6)]; [1.2 (H^2 and H^7)]	2.0055
$[Rh(\eta^5\text{-}AnCH_2C_5H_4)(\eta^2\text{-}C_8H_{14})_2]^{+\bullet}$, $\mathbf{3}^+$	283	0.2	1.02 (Rh); 5.99 (1H); 5.02 (2H); 2.77 (2H); 1.95 (2H); 1.42 (2H); 0.43 (2H); 0.38 (2H); 0.16 (2H) [5.9 (H^{10})]; [5.0 (H^{13} and H^{14})]; [2.6 (H^1 and H^8)]; [1.9 (H^3 and H^6)]; [1.3 (H^4 and H^5)]; [0.3 (H^2 and H^7)]	2.0056
$[Rh(\eta^5\text{-}AnCH_2C_5H_4)(PPh_3)_2]^{+\bullet}$, $\mathbf{4}^+$	263	0.4	3.45 (Rh); 3.46 (H^{10}); 3.19 (H^{13} and H^{14}); 3.16 (H^1 and H^8); 3.04 (H^4 and H^5); 2.54 (H^3 and H^6); 1.63 (H^2 and H^7); 1.28 (H^9)	2.0068
$[Ir(\eta^5\text{-}AnCH_2C_5H_4)(\eta^1\text{-}CO)_2]^{+\bullet}$, $\mathbf{6}^+$	268	0.4	4.27 (Ir); 5.04 (H^{10}); 2.94 (H^4 and H^5); 2.88 (H^1 and H^8); 1.55 (H^2 and H^7); 1.45 (H^3 and H^6); 1.38 (H^9); 0.95 (H^{13} and H^{14})	2.0063
$[Ir(\eta^5\text{-}AnCH_2C_5H_4)(\eta^2\text{-}C_8H_{14})_2]^{+\bullet}$, $\mathbf{7}^+$	278	0.6	0.76 (Ir); 6.14 (H^{10}); 4.54 (H^4 and H^5); 2.96 (H^1 and H^8); 1.87 (H^3 and H^4); 1.43 (H^2 and H^7)	2.0053
$[Ir(\eta^5\text{-}AnCH_2C_5H_4)(\eta^4\text{-}C_8H_{12})]^{+\bullet}$, $\mathbf{8}^+$	263	0.1	6.19 (H^{10}); 2.61 (H^1, H^4, H^5, and H^8); 2.32 (H^9); 1.61 (H^2, H^3, H^6, and H^7); 1.60 (H^{13} and H^{15}); 1.12 (H^{12} and H^{14})	2.0066

[a] In these cases spin density distribution and hyperfine coupling constants were calculated by DFT. [b] In these cases the association of hyperfine coupling constants to specific hydrogen nuclei was based upon PM3 semiempirically calculated spin density distribution.

which an anthrylic group is connected with a rhodium or iridium center (Scheme 4).

The EPR study documents clearly that a strong electronic communication exists between the athrylic moiety and the cyclopentadienylmetal subunit in the products resulting from the one-electron oxidation of complexes **1**−**8**, i.e. the cation-radicals $[M(\eta^5\text{-}AnCH_2C_5H_4)L_2]^+$. This means that the d-electrons of the metal centers are in π-symmetry orbitals and can effectively overlap with the π-orbitals of the aromatic fragment. Accordingly, DFT calculation of the spin density distribution shows clearly that, in the optimized geometry, the odd electron is delocalized over the whole molecular skeleton, the spin density distribution being the result of complex electronic effects exerted by all the molecular components as well as by molecular conformation. On this basis, it can be easily understood that the upper chemical pathway shown in the Scheme 2 will be favored when a relatively high spin density extends also over the Cp ring, while the lower reaction pathway (Scheme 2) should take place when the metal center is highly populated by the unpaired electron.

4. Experimental Details

4.1. General. The reactions and manipulations of organometallics were carried out under dinitrogen or argon using standard techniques. All solvents were dried and distilled prior to use following standard procedures. Microanalyses were performed by the Laboratorio di Microanalisi, Facoltà di Farmacia, Università di Pisa. ^{1}H NMR spectra were run at 200 MHz on a Varian Gemini 200 instrument. Infrared spectra were obtained by a FT-IR Perkin-Elmer 1750 spectrometer. Chemical ionization mass spectra (CI-MS) were obtained with Perkin-Elmer SCIEX API III. The compounds (η^5-9-anthrylmethylcyclopentadienyl)bis(η^2-ethylene)rhodium(I), **1**,[17] (η^5-9-anthrylmethylcyclopentadienyl)dicarbonylrhodium(I), **2**,[17] (η^5-9-anthrylmethylcyclopentadienyl)bis(η^2-cyclooctene)rhodium(I), **3**,[17] (η^5-9-anthrylmethylcyclopentadienyl)bis(triphenylphosphine)rhodium(I), **4**,[17] (η^5-9-anthrylmethylcyclopentadienyl)(η^4-1,5-cyclooctadiene)rhodium(I), **5**,[14] (η^5-9-anthrylmethylcyclopentadienyl)bis(η^2-cyclooctene)iridium(I), **7**,[17] (η^5-9-anthrylmethylcyclopentadienyl)(η^4-1,5-cyclooctadiene)iridium(I), **8**,[17] (η^5-cyclopentadienyl)dicarbonylrhodium(I),[31] 9-anthrylmethylcyclopentadienylthallium(I),[17] di-μ-chlorotetrakis(carbonyl)dirhodium(I),[32] and chlorodicarbonyl(p-toluidine)-iridium(I)[33] were prepared as reported.

4.2. Electrochemical Measurements. The one-compartment electrochemical cell was of airtight design with high-vacuum glass stopcocks fitted with either Teflon or Kalrez (DuPont) O-rings in order to prevent contamination by grease. The connections to the high-vacuum line and to the Schlenck containing the solvent were obtained by spherical joints also fitted with Kalrez O-rings. The pressure in the electrochemical cell, prior to performing the trap-to-trap distillation of the solvent, ranged typically from 1.0 to 2.0 $\times$ 10^{-5} mbar. The working electrode consisted of either a 0.6 mm diameter platinum wire (0.15 cm^2 approximately) sealed in glass or a platinum disk microelectrode (r = 125 μm) also sealed in glass. The counter electrode consisted of a platinum spiral, and the quasi-reference electrode was a silver spiral. The quasi-reference electrode drift was negligible for the time required by a single experiment. Both the counter and the reference electrode were separated from the working electrode by ~0.5 cm. Potentials were measured with the ferrocene standard and are always referred to the saturated calomel electrode (SCE). $E_{1/2}$ values correspond to $(E_{pc} + E_{pa})/2$ from CV. For irreversible

(31) Fischer, E. O.; Fischer, R. D. *Z. Naturforsch. B* **1961**, *16*, 475.
(32) McCleverty, J. A.; Wilkinson, G. *Inorg. Synth.* **1966**, *8*, 211.
(33) Klablunde, U. *Inorg. Synth.* **1974**, *15*, 82.

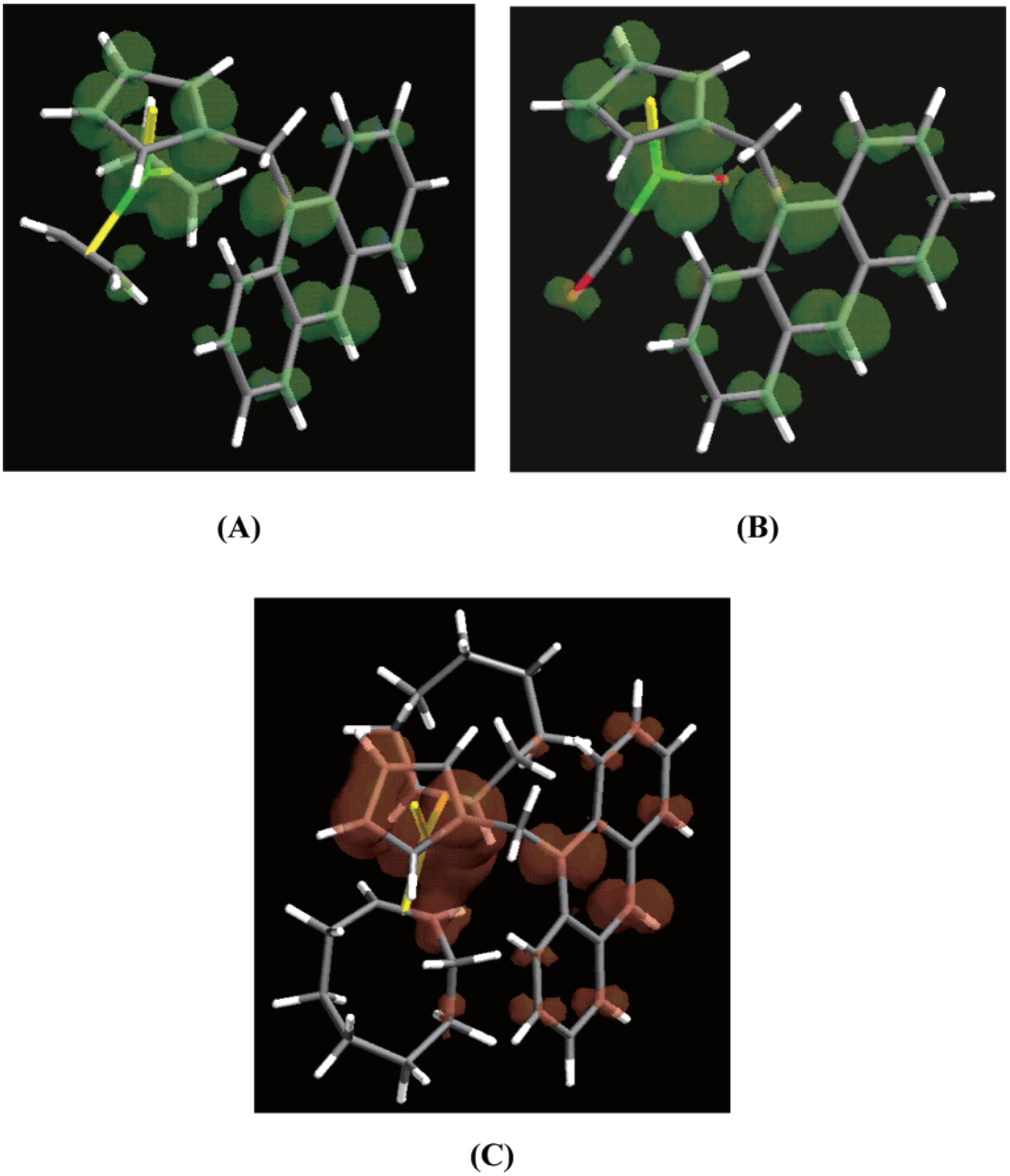

Figure 5. DFT calculated spin density surface (0.001 electron/au^3) of the cations $[Rh(\eta^5\text{-}AnCH_2C_5H_4)(\eta^2\text{-}C_2H_4)_2]^{+\bullet}$, **1**$^+$ (A), $[Rh(\eta^5\text{-}AnCH_2C_5H_4)(\eta^1\text{-}CO)_2]^{+\bullet}$, **2**$^+$ (B), and $[Rh(\eta^5\text{-}AnCH_2C_5H_4)(\eta^2\text{-}C_8H_{14})_2]^{+\bullet}$, **3**$^+$ (C).

peaks, the peak potential, E_p, is given, measured at 0.5 V s^{-1}. Ferrocene was also used as an internal standard for checking the electrochemical reversibility of a redox couple. Voltammograms were recorded with an AMEL Model 552 potentiostat or a custom-made fast potentiostat controlled by either an AMEL Model 568 function generator or an ELCHEMA Model FG-206F. Data acquisition was performed by a Nicolet Model 3091 digital oscilloscope interfaced to a PC. Temperature control was accomplished within 0.1 °C with a Lauda RL 6 CS thermostat. Digital simulation of the CV curves was carried out by using the DigiSim 3.0 software by Bioanalytical Systems Inc. All the electrochemical steps were considered fast in the simulation, and the chemical rate constants were chosen so as to obtain a visual best fit over a 10^2-fold range of scan rates.

4.3. EPR Measurements. The X-band EPR spectra were obtained by a Varian E112 spectrometer controlling the temperature by an OXFORD EPR 900 cryostat. The EPR spectrometer was interfaced to an IPC 610/P566C industrial grade Advantech computer by means of a data-acquisition system consisting of an acquisition board capable of acquiring up to 500 000 12-bit samples per second including 32-bit add to memory, thus giving on-line signal averaging,[34] and a software package specially designed for EPR experiments.[35] The EPR spectra were run by placing the sample (typically 15−20 μL) into quartz tubes (external diameter, 3 mm; internal diameter, 2 mm) fitted with a quartz-Pyrex joint and a Bibby Quickfit Rotaflo PTFE tap (Disa, Milan), according to already published procedures.[23] All the EPR experiments were run in a 1:1 (v/v) 1,1,1,3,3,3-hexafluoro-2-propanol/dichloromethane mixture. Both solvents were saturated with argon before use.

(34) Ambrosetti, R.; Ricci, D. *Rev. Sci. Instrum.* **1991**, *62*, 2281.
(35) Pinzino, C.; Forte, C. EPR-ENDOR, ICQEM-CNR Rome, Italy, 1992.
(36) Maggini, M.; Guldi, P. M.; Mondini, S.; Scorrano, S.; Paolucci, F.; Ceroni, P.; Roffia, S. *Chem. Eur. J.* **1998**, *4*, 1992, and references therein.

Scheme 4

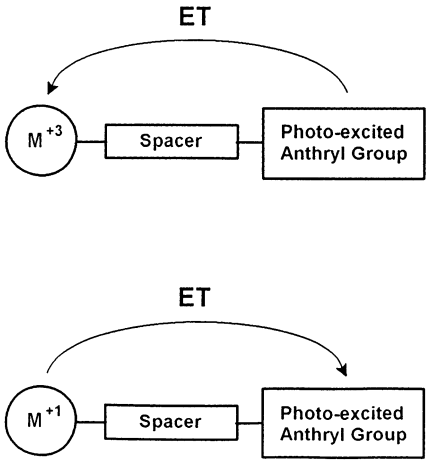

4.4. (η^5-9-Anthrylmethylcyclopentadienyl)dicarbonyliridium(I), 6. A mixture of 9-anthrylmethylcyclopentadienylthallium(I) (0.46 g, 1.0 mmol), chlorodicarbonyl(pyridine)-iridium(I) (0.36 g, 1.0 mmol), and benzene (35 mL) was stirred at room temperature for 24 h and then filtered. The solution was dried under reduced pressure. The residue was dissolved in benzene (2 mL) and purified by column (internal diameter, 10 mm; length, 30 mm) chromatography on alumina (aluminum oxide 90, 70−230 mesh, Merck), using a benzene/*n*-hexane mixture (8:2, v/v) as eluant. From the first orange-yellow band that eluted, 0.30 g of **6** (60%, yield) was obtained, as an ochre-yellow oily compound that crystallizes on standing at room temperature. Found: C, 52.4; H, 2.9. Anal. Calcd for $C_{22}H_{15}O_2Ir$: C, 52.47; H, 3.00. CI-MS, *m*/*z* (relative intensity %): 503 (^{191}Ir) $[M + H]^+$, 505 (^{193}Ir) $[M + H]^+$. IR (benzene solution, cm^{-1}): 2924 (s), 2853 (s), 2027 (s), 1957 (s), 1618 (s), 1452 (s), 1330 (s), 1035 (s), 812 (s). ^{1}H NMR (C_6D_6): δ 8.10 (d, 2H, J = 6 Hz, 9-anthryl), 8.04 (s, 1H, 9-anthryl), 7.77 (d, 2H, J = 6 Hz, 9-anthryl), 7.33−7.28 (m, 4H, 9-anthryl), 4.71 (d, 2H, J = 3 Hz, η-C_5H_4), 4.54 (d, 2H, J = 3 Hz, η-C_5H_4), 4.32 (s, 2H, CH_2) ppm.

Acknowledgment. We thank Dr. A. Raffaelli (CNR, Pisa, Italy) for the measurement of the mass spectrum of complex **6**. Financial supports from MIUR (Rome, Italy) and from the University of Bologna (Funds for Selected Research Topics) are kindly acknowledged.

OM020607J